

Line and rotational defects in boron-nitrene: Structure, energetics, and dependence on mechanical strain from first-principles calculations

Dmitry G. Kvashnin^{1,2}, Pavel B. Sorokin^{1,2,3}, Dmitry Shtansky¹, Dmitri Golberg⁴, and Arkady V. Krasheninnikov^{*5}

¹National University of Science and Technology MISiS, 4 Leninskiy Prospekt, Moscow 119049, Russian Federation

²Moscow Institute of Physics and Technology, 9 Institutsky Lane, Dolgoprudny 141700, Russian Federation

³Technological Institute for Superhard and Novel Carbon Materials, 7a Centralnaya Street, Troitsk, Moscow 142190, Russian Federation

⁴World Premier International Center (WPI) for Materials Nanoarchitectonics (MANA), National Institute for Materials Science (NIMS), Namiki 1-1, Tsukuba 3050044, Ibaraki, Japan

⁵Department of Applied Physics, Aalto University, P.O. Box 11100, FI-00076 Aalto, Finland

Received 21 November 2014, revised 15 February 2015, accepted 16 February 2015

Published online 16 March 2015

Keywords first-principles calculations, *h*-BN monolayers, mechanical strain, point defects, thermodynamics

*Corresponding author: e-mail arkady.krasheninnikov@aalto.fi, Phone: +358504333260, Fax: +35898554019

A new class of point defects was recently discovered in sheets of non-stoichiometric transition metal dichalcogenides, two-dimensional (2D) materials with a trigonal prismatic lattice. Using *ab initio* calculations, we study the morphology and energetics of such defects, which involve 60° rotations of covalent bonds, in another 2D material with the same symmetry—hexagonal BN monolayer. We further investigate transformations of isolated vacancies into rotational defects and vacancy lines and demonstrate that agglomeration of

vacancies is energetically favorable, but lines are preferable over rotational defects in the case of B-vacancies, while these defects have similar energies in N-deficient sheets. Finally, we study effects of mechanical strain on defect energetics. Our results provide microscopic insights into the thermodynamics of defects and point towards new routes to the engineering of the properties of boron-nitrene by introduction of defects and strain.

© 2015 WILEY-VCH Verlag GmbH & Co. KGaA, Weinheim

1 Introduction Following the fabrication of free-standing graphene [1], the rapidly growing family of two-dimensional (2D) materials have been at the forefront of the research, as the reduced dimensionality provides ample opportunities for developing materials with unique characteristics. Among 2D systems, *hexagonal* boron nitride (*h*-BN or boron-nitrene) [2, 3] which contrary to graphene has no direct analogues in nature and can only be manufactured synthetically, has attracted enormous amount of attention from the materials science community. Insulating electronic properties in combination with high mechanical stiffness and thermal stability suggest using *h*-BN in a plethora of applications [2], for example as a substrate in 2D electronic devices.

At the same time, the 2D nature of boron-nitrene implies that intrinsic and extrinsic defects in this material should

have a stronger effect on its properties and makes *h*-BN more vulnerable to the effects of the environment, as compared to bulk systems. Indeed, numerous [4–8] studies confirmed the presence of point and line defects in *h*-BN sheets. Even though some of these defects may have been introduced during the characterization of the material by transmission electron microscopy (TEM) [6, 7, 9, 10], the complete control over boron-nitrene properties requires the detailed microscopic knowledge of defect behavior and properties, i.e., the information on their atomic structure, as well as their formation and migration energies. Moreover, it is well known that defects, especially irradiation-induced ones [11], can be useful for achieving specific functionalities of BN nanostructures, e.g., sidewall functionalization [12] of BN nanotubes or local magnetism in BN

layers [13], which further motivates research on defect properties.

The behavior of single vacancies in both B and N sublattices has been extensively studied [6–8, 14, 15], see also Ref. [16] and references therein. As their formation energy is quite high [14, 17–20], such defects are expected not to be present in BN nanostructures in measurable concentrations at room temperature, but can be produced by an electron beam of the microscope, and likely disappear later by picking up carbon atoms from the environment [21–23]. Another type of point defects, which can be produced by a 90° rotation of a bond in the atomic network of *h*-BN and are referred to as Stone–Wales defects [24], Figure 1(a and b) has widely been discussed, but it has never been observed, though. Such defects do exist in graphene [25] and silica bilayers [26], 2D systems with the hexagonal symmetry. In *h*-BN, a system with the trigonal symmetry, such defects would require homo-nuclear bonds, which normally are energetically unfavorable.

Recently, a new class of rotational defects has been observed in single layer transition metal dichalcogenides (TMDs) [27], such as WS₂ and WSe₂, 2D materials with the trigonal symmetry, the same as in boron-nitrene. The heteroatomic nature of chemical bonds was preserved by a 60° rotation of several atoms around their common neighboring atom, as schematically shown in Fig. 1(c and d) for boron-nitrene. Note that transformations involve six

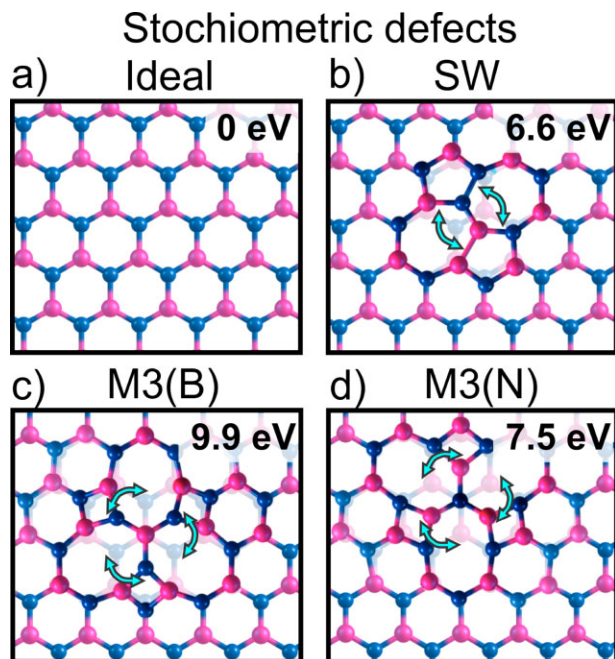


Figure 1 Atomic structures of stoichiometric rotational defects in *h*-BN monolayer. SW corresponds to a Stone–Wales defect formed by a 90° rotation of a bond. M3 stands for a 60° rotation of three atoms. Formation energies of defects are also listed.

atoms in TMDs, and three in BN sheets. Such defects appeared in some chalcogen-deficient TMDs at high temperatures due to coalescence of single vacancies, and were energetically favorable with respect to isolated vacancies. However, in some TMD materials, e.g., MoS₂, line agglomerations of vacancies had lower energies as compared to large rotational defects [28]. Such observations naturally give rise to the following questions: “*Can such defects exist in h-BN, and can they appear due to vacancy agglomeration, as in TMDs?*”

Here, by employing first-principles calculations, we study the energetics of rotational and line vacancy defects in *h*-BN. We further investigate the behavior of the defects under the influence of mechanical strain. We analyze the strain fields near point defects and show that the strain generated by single vacancy defects (SV) can be reduced by coalescence of SVs to complex defects like divacancy (DV) or line defects. Our results indicate that rotational defects are higher in energy than line defects in B-deficient boron-nitrene, and should not exist in *h*-BN under ambient conditions. However, rotational and line defects have similar energies in N-deficient *h*-BN, and they should even become energetically favorable under mechanical strain, pointing towards new defect and strain-mediated routes to engineering the properties of boron-nitrene.

2 Method and model Our calculations were performed within the framework of density functional theory [29, 30] using the generalized gradient approximation with the Perdew–Burke–Ernzerhof [31] parameterization as implemented in the Vienna *ab initio* Simulation Package [32–34]. The projected augmented wave (PAW) [35] approach was employed to describe core electrons, and a plane wave basis set with energy cutoff of 400 eV was used. To calculate atomic structure, the Brillouin zone was sampled according to the Monkhorst–Pack [36] scheme with a *k*-point density of 0.08 Å⁻¹. To avoid spurious interactions between neighboring images in the supercell approach, a vacuum layer of 12 Å in the transverse directions was included. Atomic structure optimization was performed until the forces acting on each atom became less than 0.05 eV/Å. *h*-BN was modeled as a supercell composed from 12 × 12 unit cells, so that the initial structure, in which the defects were introduced, consisted of 288 atoms. To assess the errors in the formation energies of defects, we also carried out calculations for B/N vacancies and M3 rotational defects in a 14 × 14 supercell composed from 392 atoms and found that the difference in the formation energies was less than 0.15 eV as compared to the results obtained for the 12 × 12 supercell. This difference is substantially less than the typical difference (more than 1 eV) between formation energies of defects we compare, e.g., three single vacancies and the M3 rotational defect. For large line defects, we performed another test, we calculated the formation energy of such defects with and without supercell optimization. Such calculations should give a lower and an upper limit on the formation energy of

the defect in the dilute limit. For Line B/N SV5 defects, we found that the difference between the results is 0.6 and 0.7 eV, respectively, which is again considerably less than the typical values of energy difference between line and rotational defects, so that our conclusion are at least qualitatively correct.

3 Results and discussion Hexagonal boron nitride monolayers can contain stoichiometric (formed by the rotation of B–N bonds) and nonstoichiometric (with some atoms missing) defects, which can be constructed from vacancies. We found that in the former case formation of Stone–Wales defects [90° bond rotation, Fig. 1(b)] requires relatively high energy of about 6.6 eV, indicating that indeed their concentration even at high temperatures of 1000°C should be negligible.

Their formation energies, calculated as a difference in total energies of the system with and without defects for M3 rotational defects (where M3 stands for rotation of three bonds around their common center) are also shown in Fig. 1. It is evident that formation energies of M3 rotational defects are higher than for the SW defect, even though the heteroatomic nature of the bonds is preserved.

To understand the reason for such a behavior, we calculated strain fields near the defects. Strain fields were defined as a difference between the B–N bond lengths in the system with defects and in pristine one [37]. All defects gave rise to long-ranged strain fields, see Fig. 2(a–c). The introducing of low-symmetry SW defect [Fig. 1(b)] leads to

the formation of the regions of compressed B–N bonds from the side of pentagonal rings and stretched bonds from the side of heptagonal rings.

The M3 defects presented in Fig. 2(b) and (c) were formed from the pristine structure by the rotation of three boron/nitrogen atoms with respect to nitrogen/boron, respectively. Threefold symmetry of such type of defects affects the strain field in the same manner, so that the strain field also has threefold symmetry.

Large strain fields near defects indicate that their formation energy can considerably change if the external stress is applied. We calculated the dependence of the formation energy on bi-axial tensile strain [Fig. 2(d)] using the relation $E_f(\epsilon) = E_{\text{def}}(\epsilon) - E_{\text{prist}}(\epsilon)$ where E_{def} and E_{prist} are energies of defective and pristine configurations, respectively. The dependence of the total energy on strain and overall the mechanical properties of the pristine system agreed well with the previous calculations [38]. We found a monotonous and rather weak dependence of formation energy on strain, so that one cannot expect any changes in atomic structure of *h*-BN monolayer at least in the strain range upto 5%. The formation energies for all the defects decrease with strain indicating reduced radiation hardness, as reported before [39].

Having assessed the energetics of defects in the stoichiometric boron-nitrene, we moved on to defects in the non-stoichiometric *h*-BN sheets. The behavior of defects in the atom-deficient system (either B or N atoms missing) is more complicated, as compared to stoichiometric defects.

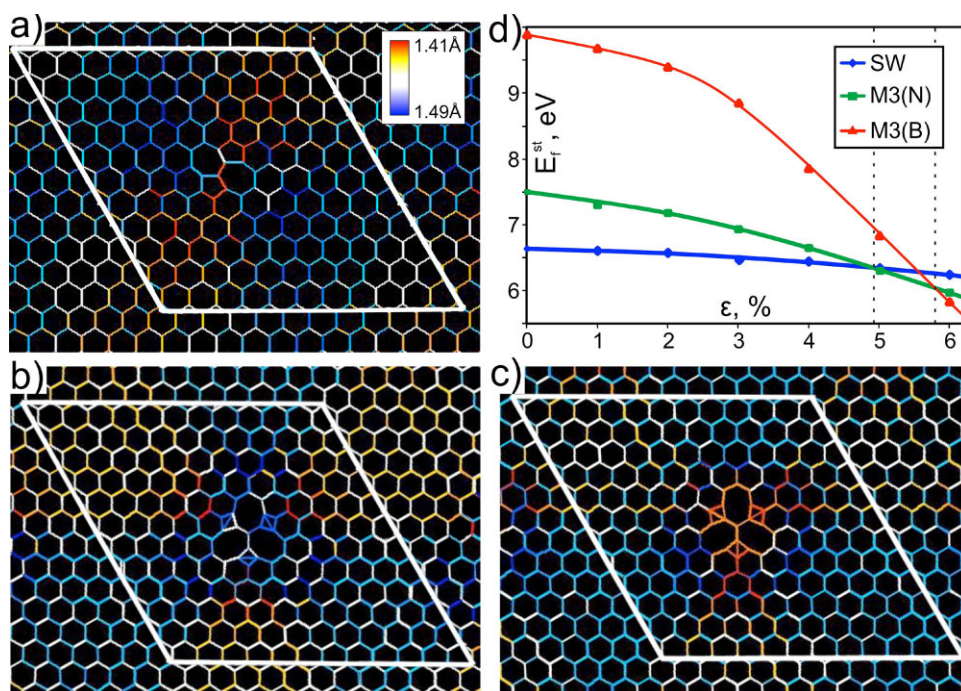


Figure 2 Strain fields near rotational defects in boron-nitrene. SW defect (a), defects caused by the rotation of three boron/nitrogen atoms with respect to nitrogen/boron, respectively (b, c). Formation energy as a function of bi-axial strain (d); the crossing points are denoted by vertical lines. The bonds are colored according to an increase (blue) or decrease (red) in the bond length.

The creation of SVs also incurs a high energy penalty (>7.8 eV). We stress that the formation energy depends on the environment, that is the chemical potentials of the atoms involved [40] and the charge state of the defect, but in any case, vacancies can be produced by the electron beam. Once formed, SVs cannot be healed just due to the lack of atoms (at least for the *in vacuo* case). Finite migration barriers [41] allow vacancies to diffuse (at high temperatures) and coalescence with each other forming either line or rotational defects. Therefore SVs can be considered as building blocks for new defects in the *h*-BN, with their formation energy being dependent upon external conditions. We note that at low temperatures when diffusion is suppressed, formation of triangular holes [6, 7] under electron beam is expected, though.

In order to understand if coalescence of vacancies into larger defects is possible and what kinds of defects

(rotational or line defects) are favorable, we calculated the energy difference E_c between defect agglomerations (that is rotational or line structures) and corresponding isolated defects and normalized them over the number of missing atoms. E_c can be referred to as the energy released upon coalescence of defects. We also accounted for the effects of tensile bi-axial strain on the energetics.

The calculated dependencies of coalescence energy on strain are presented in Fig. 3. The number of missing atoms is also given. The considered rotational defects were the M3 and M5 defects, which involved rotations of three and seven atoms around one and three centers, see Ref. [27] for details. The negative values of formation energies indicate that coalescence of defects is energetically favorable. It is also evident from Fig. 3(b) that even short line defects composed from three B vacancies have lower energy than the rotational defects, and external strain does not give rise to any changes in

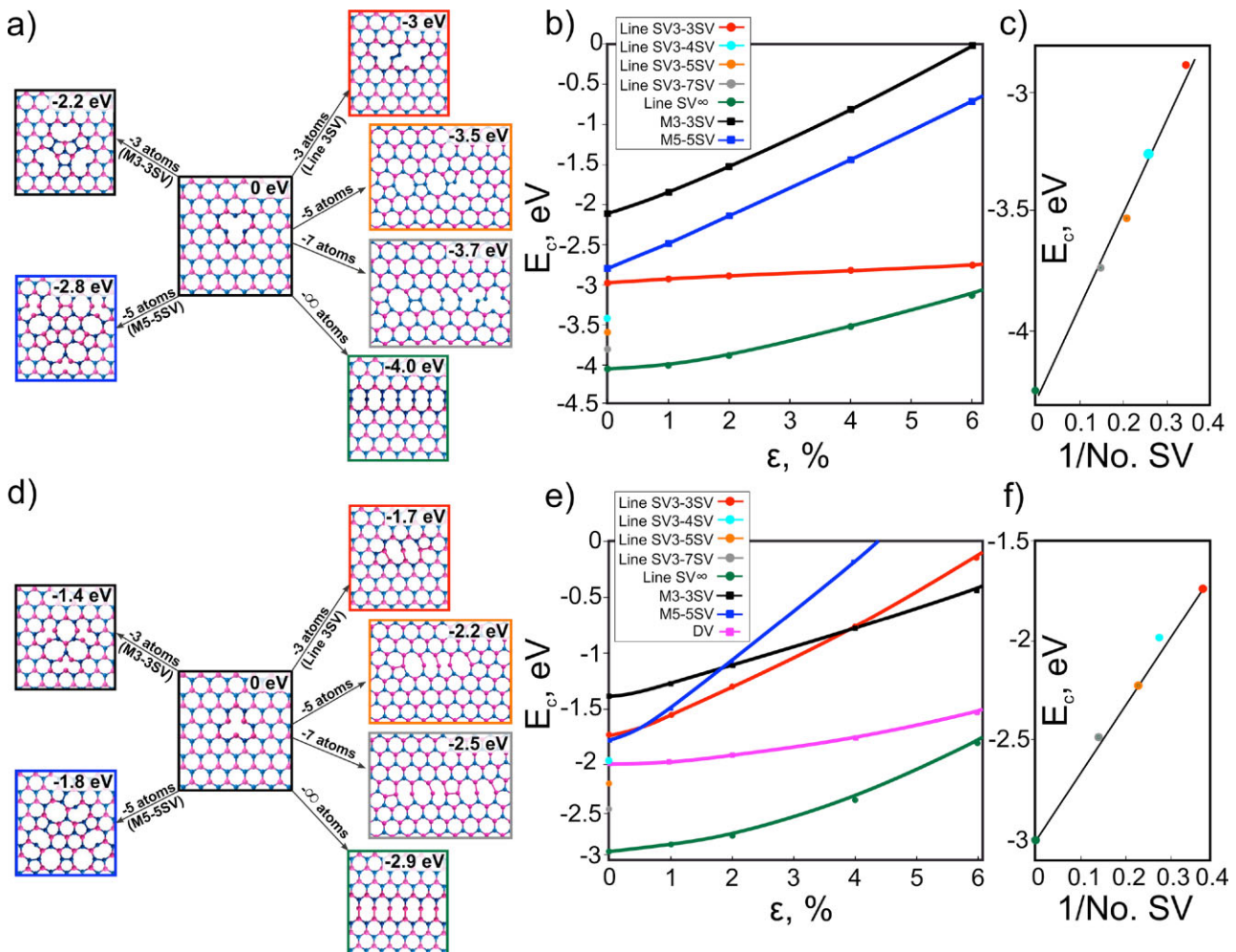


Figure 3 (a,d) Atomic structures of complex defects in the non-stoichiometric (a) B- and (d) N-deficient *h*-BN sheet. The energies released upon coalescence of isolated vacancies are shown in red in each panel. (b,e) Dependence of coalescence energy of the defects in (b) B- and (e) N-deficient *h*-BN sheet upon bi-axial strain. Di-vacancy defect, rotational defects M3-3SV and M5-5SV are marked in pink, black, and blue, respectively, linear defects consisted of three, four, five, and seven missed atoms are marked in red, cyan, orange, and gray, respectively, whereas the energy for infinite line of vacancies is depicted in green. (c,f) The dependence of the coalescence energy of line defects on the inverse length of the defects for the zero external strain.

the picture. Similar trends have been observed in S-deficient MoS₂ samples [28]. In panels c and f, the dependence of the coalescence energy of line defects on the inverse length of the defects is shown for the zero external strain.

The situation is more complicated for the N-deficient case. The energies of line and rotational defects are very close, so that one can expect that defects of either kind can appear. Moreover, their concentration can be controlled by strain. Divacancies, which involve both N and B vacancies, can also appear, but the type of vacancies can generally be controlled by altering chemical potentials of B/N atoms, that is by the environment (e.g., by putting the system in a N- or B-rich atmosphere).

Further 60° rotations should give rise to larger defects, as in TMDs [27]. It is evident already from the M5-5SV defect that the 5-8-5 line is actually a boundary separating grains with a twin mirror symmetry. The defects can further grow up through bond rotations, and correspondingly the area of the phase with the mirrored symmetry decreases. The 5-8-5 lines are exactly the structures, which have been discussed in the literature as extended defects for engineering the electronic properties of *h*-BN sheets and ribbons [42]. In agreement with previous calculations (for the ribbon geometry with edges of the ribbons passivated with H-atoms), our results indicate that such defect indeed give rise to new states in the gap of boron-nitrene.

Figure 4 shows the electronic structure of the 5-8-5 grain boundary in *h*-BN simulated by reflected zigzag-edge ribbons due to mirror symmetry induced by the defect. The defect-induced states are clearly evident. A similar behavior was reported for the 5-7 dislocation [43], 8-5-5-8 boundary in MoS₂ [44], WSe₂ [27], and epitaxial graphene on Ni(111) [45]. For the boundary formed by B dimers, a new state appears in the vicinity of the conduction band, while in the opposite case occupied states are formed close to the valence bands. We stress that DFT calculations with semilocal exchange and correlation functionals underestimate the gap, as evident from more accurate GW

calculations [46] but give a qualitatively correct picture of defect states in this material [47].

4 Conclusions To sum up, using first-principles atomistic calculations carried out within the framework of the density-functional theory, we studied the morphology and energetics of rotational and line defects in boron-nitrene—a 2D material with a trigonal prismatic lattice—and tried to find analogies with the behavior of such defects in 2D TMDs, 2D systems with the same crystal lattice symmetry. We showed that the agglomeration of isolated vacancies into the rotational and line defects is energetically favorable, but lines are preferable over rotational defects in the case of B-vacancies, while these defects have similar energies in N-deficient sheets. The behavior of defects in *h*-BN is reminiscent of that in MoS₂, but different from what has been observed in other TMDs [27]. We also studied the effects of mechanical strain on defect energetics and showed that defect types and their abundance can be controlled by strain in the case of N-deficient BN sheets. Our results provide microscopic insights into the behavior of defects, and indicate that defect agglomeration may be observed in BN sheets using high-resolution TEM at high temperature, which should allow defect migration and atomic structure transformations. The B or N deficit can be created by electron-beam-induced knock-on damage and possibly selection of pressure of the species in the chamber. As line and rotational defects give rise to different defect-induced states in the electronic structure of *h*-BN, our findings point towards new defect and strain-mediated routes to engineering the properties of boron-nitrene. Our first-principles results should also be useful for the development and testing empirical potentials for BN structures: there has recently been a lot of interest in classical Tersoff-like potentials [16, 48] for the BN systems, and the accurate values of defects formation energies can be used for the validation of empirical potential results [16, 49].

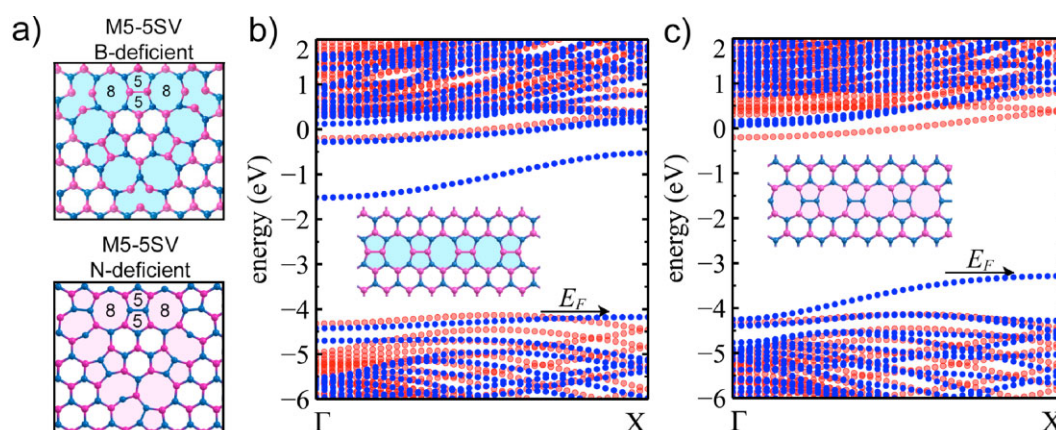


Figure 4 Atomic structures of the 5-8-5 lines, which are the boundaries between *h*-BN structures with mirrored symmetry by the example of M5 defects (a) and infinite lines (insets in panels b and c). Electronic structure of 5-8-5 line defect in (b) boron and (c) nitrogen deficient case in *h*-BN ribbons. The red plots are the data for the ribbons without line defects. Fermi level is marked by the arrow.

Acknowledgements The work was carried out with partial financial support from the Ministry of Education and Science of the Russian Federation in the framework of Increase Competitiveness Program of NUST “MISiS” (no. 3-2014-010). D.G.K. and P.B.S. gratefully acknowledge the financial support from the Ministry of Education and Science of the Russian Federation (state task no. 11.1077.2014/K). D.S. and D.G. also acknowledge a funding from the Ministry of Education and Science of the Russian Federation (“Mega-Grant” award, No. 11.G34.31.0061 and Increase Competitiveness Program of NUST (MISiS), No. K2-2015-001). A.V.K. also acknowledges financial support from the Academy of Finland through project no. 263416. P.B.S. acknowledges the Grant of President of Russian Federation for government support of young PhD scientists (MK-6218.2015.2). We are grateful to the “Chebishev” and “Lomonosov” supercomputers of Moscow State University and the Joint Supercomputer Center of the Russian Academy of Sciences for the possibility of using a cluster computer for our calculations. We further thank CSC IT Center for Science Ltd. for generous grants of computer time.

References

- [1] M. H. Gass, U. Bangert, A. L. Bleloch, P. Wang, R. R. Nair, and A. K. Geim, *Nature Nanotechnol.* **3**, 676 (2008).
- [2] D. Golberg, Y. Bando, Y. Huang, T. Terao, M. Mitome, C. Tang, and C. Zhi, *ACS Nano* **4**, 2979 (2010).
- [3] L. Song, L. Ci, H. Lu, P. B. Sorokin, C. Jin, J. Ni, A. G. Kvashnin, D. G. Kvashnin, J. Lou, B. I. Yakobson, and P. M. Ajayan, *Nano Lett.* **10**, 3209 (2010).
- [4] N. Alem, O. V. Yazyev, C. Kisielowski, P. Denes, U. Dahmen, P. Hartel, M. Haider, M. Bischoff, B. Jiang, S. G. Louie, and A. Zettl, *Phys. Rev. Lett.* **106**, 126102 (2011).
- [5] O. Cretu, Y. C. Lin, and K. Suenaga, *Nano Lett.* **14**, 1064 (2014).
- [6] C. Jin, F. Lin, K. Suenaga, and S. Iijima, *Phys. Rev. Lett.* **102**, 195505 (2009).
- [7] J. C. Meyer, A. Chuvilin, G. Algara-Siller, J. Biskupek, and U. Kaiser, *Nano Lett.* **9**, 2683 (2009).
- [8] K. Suenaga, H. Kobayashi, and M. Koshino, *Phys. Rev. Lett.* **108**, 075501 (2012).
- [9] A. L. Gibb, N. Alem, J. H. Chen, K. J. Erickson, J. Ciston, A. Gautam, M. Linck, and A. Zettl, *J. Am. Chem. Soc.* **135**, 6758 (2013).
- [10] J. Kotakoski, C. H. Jin, O. Lehtinen, K. Suenaga, and A. V. Krasheninnikov, *Phys. Rev. B* **82**, 4 (2010).
- [11] A. V. Krasheninnikov and F. Banhart, *Nature Mater.* **6**, 723 (2007).
- [12] X. J. Dai, Y. Chen, Z. Chen, P. R. Lamb, L. H. Li, J. du Plessis, D. G. McCulloch, and X. Wang, *Nanotechnology* **22**, 245301 (2011).
- [13] E. Machado-Charry, P. Boulanger, L. Genovese, N. Mousseau, and P. Pochet, *Appl. Phys. Lett.* **101**, 132405 (2012).
- [14] S. Azevedo, J. R. Kaschny, C. M. C. de Castilho, and F. de Brito Mota, *Eur. Phys. J. B* **67**, 507 (2009).
- [15] W. H. Moon and H. J. Hwang, *Phys. Lett. A* **320**, 446 (2004).
- [16] A. V. Krasheninnikov and K. Nordlund, *J. Appl. Phys.* **107**, 071301 (2010).
- [17] S. Okada, *Phys. Rev. B* **80**, 161404(R) (2009).
- [18] G. J. Slotman and A. Fasolino, *J. Phys.: Condens. Matter* **25**, 045009 (2012).
- [19] L. C. Yin, H. M. Cheng, and R. Saito, *Phys. Rev. B* **81**, 153407 (2010).
- [20] B. Huang and H. Lee, *Phys. Rev. B* **86**, 245406 (2012).
- [21] N. Berseneva, A. V. Krasheninnikov, and R. M. Nieminen, *Phys. Rev. Lett.* **107**, 035501 (2011).
- [22] X. Wei, M. S. Wang, Y. Bando, and D. Golberg, *ACS Nano* **5**, 2916 (2011).
- [23] O. L. Krivanek, M. F. Chisholm, V. Nicolosi, T. J. Pennycook, G. J. Corbin, N. Dellby, M. F. Murfitt, C. S. Own, Z. S. Szilagy, M. P. Oxley, S. T. Pantelides, and S. J. Pennycook, *Nature* **464**, 571 (2010).
- [24] A. J. Stone and D. J. Wales, *Chem. Phys. Lett.* **128**, 501 (1986).
- [25] F. Banhart, J. Kotakoski, and A. V. Krasheninnikov, *ACS Nano* **5**, 26 (2011).
- [26] T. Björkman, S. Kurasch, O. Lehtinen, J. Kotakoski, O. V. Yazyev, A. Srivastava, V. Skakalova, J. H. Smet, U. Kaiser, and A. V. Krasheninnikov, *Sci. Rep.* **3**, 3482 (2013).
- [27] Y. C. Lin, T. Björkman, H. P. Komsa, F. S. Huang, C. H. Yeh, K. H. Lin, J. Jadcak, Y. S. Huang, P. W. Chiu, and A. V. Krasheninnikov, and K. Suenaga, *Nature Commun.*, DOI: 10.1038/ncomms7736 (2015).
- [28] H. P. Komsa, S. Kurasch, O. Lehtinen, U. Kaiser, and A. V. Krasheninnikov, *Phys. Rev. B* **88**, 035301 (2013).
- [29] P. Hohenberg and W. Kohn, *Phys. Rev.* **136**, B864 (1964).
- [30] W. Kohn and L. J. Sham, *Phys. Rev.* **140**, A1133 (1965).
- [31] J. P. Perdew, K. Burke, and M. Ernzerhof, *Phys. Rev. Lett.* **77**, 3865 (1996).
- [32] G. Kresse and J. Hafner, *Phys. Rev. B* **47**, 558 (1993).
- [33] G. Kresse and J. Hafner, *Phys. Rev. B* **49**, 14251 (1994).
- [34] G. Kresse and J. Furthmüller, *Phys. Rev. B* **54**, 11169 (1996).
- [35] P. E. Blöchl, *Phys. Rev. B* **50**, 17953 (1994).
- [36] H. J. Monkhorst and J. D. Pack, *Phys. Rev. B* **13**, 5188 (1976).
- [37] A. V. Krasheninnikov and R. M. Nieminen, *Theor. Chem. Acc.* **129**, 625 (2011).
- [38] Q. Peng, W. Ji, and S. De, *Comput. Mater. Sci.* **56**, 11 (2012).
- [39] Q. Peng, W. Ji, and S. De, *Nanoscale* **5**, 695 (2013).
- [40] C. Freysoldt, B. Grabowski, T. Hickel, J. Neugebauer, G. Kresse, A. Janotti, and Van de Walle, *Rev. Mod. Phys.* **86**, 253 (2014).
- [41] A. Zobelli, C. P. Ewels, A. Gloter, and G. Seifert, *Phys. Rev. B* **75**, 094104 (2007).
- [42] X. Li, X. Wu, X. C. Zeng, and J. Yang, *ACS Nano* **6**, 4104 (2012).
- [43] Z. Zhang, X. Zou, V. H. Crespi, and B. I. Yakobson, *ACS Nano* **7**, 10475 (2013).
- [44] A. N. Enyashin, M. Bar-Sadan, L. Houben, and G. Seifert, *Condens. Matter Mater. Sci.* **117**, 10842 (2013).
- [45] J. Lahiri, Y. Lin, P. Bozkurt, I. I. Oleynik, and M. Batzill, *Nature Nanotechnol.* **5**, 326 (2010).
- [46] L. Wirtz, A. Marini, and A. Rubio, *Phys. Rev. Lett.* **96**, 126104 (2006).
- [47] N. Berseneva, A. Gulans, A. V. Krasheninnikov, and R. M. Nieminen, *Phys. Rev. B* **87**, 035404 (2013).
- [48] K. Albe, W. Möller, and K. H. Heiniga, *Radiat. Eff. Defects Solids* **141**, 85 (1997).
- [49] O. Lehtinen, E. Dumur, J. Kotakoski, A. V. Krasheninnikov, K. Nordlund, and J. Keinonen, *Nucl. Instrum. Methods Phys. Res. B* **269**, 1327 (2011).